

Resonant dielectric waveguide-based nanostructure for efficient interaction with color centers in nanodiamonds

O. N. Sergaeva, I. A. Volkov, R. S. Savelev

ITMO University, St. Petersburg 197101, Russia

r.savelev@metalab.ifmo.ru

PACS 42.25.Fx, 42.79.-e, 42.82.Gw

DOI 10.17586/2220-8054-2019-10-3-266-272

Diamond nanoparticles containing single color centers are considered to be one of the most promising realizations of the sources of single photons required for many potential applications in quantum telecommunication and quantum computing systems. Their implementation in practical schemes, however, requires a sufficient increase in their brightness, including the enhancement of both emission and collection efficiency. In this work, we propose a design of a compact planar structure composed of a dielectric periodic cavity coupled with a strip waveguide that is particularly suitable for improving optical characteristics of color centers embedded in a nanodiamond placed inside the structure. We numerically demonstrate that such scheme permits the achievement of simultaneous increase of emission rate of color centers by ≈ 50 times in a spectral range ≈ 2 nm, and up to $\approx 85\%$ out-coupling efficiency of emission to the dielectric strip waveguides. We analyze the main factors that decrease the performance of the proposed arrangement and discuss the possible ways for restoring it.

Keywords: nanodiamonds, color centers, dielectric cavity, Purcell effect, zero-phonon-line emission.

Received: 9 May 2019

Color centers in diamonds are recognized as one of the most propitious platforms for development of single photon sources [1,2], for creating nanoscale sensors [3], for magnetometry [4,5], and thermometry [6,7] due to the possibility of their manipulation at room temperature and quite long electronic spin coherence times. The main problem that prevents their implementation in practical schemes is their relatively low brightness, i.e., the number of photons that a defect emits in a certain period of time, and that can be further collected, is relatively small [2].

The brightness of a source is determined by several factors: its luminescence rate, emission collection efficiency, internal quantum efficiency of the source and radiative efficiency of the surrounding environment. Moreover, creation of coherent sources of indistinguishable single photons based on color centers for quantum applications requires them to emit predominantly into the zero phonon line (ZPL), while, for instance, for negatively charged NV centers at room temperature about 96% of the energy is emitted through the phonon side-band [1]. Some other types of color centers, e.g., SiV⁻ defects, exhibit much higher fraction of ZPL emission, however, they suffer from low internal quantum efficiency [1,8]. Another essential problem is the efficient collection of the luminescence. For instance, the fraction of emission from color centers in bulk diamond or diamond films that can be detected by a confocal microscope is limited by only several percents due to high refractive index contrast between the diamond and vacuum. Emission from color centers in nanodiamonds does not suffer from such a problem, but being dipole-like in nature, it slightly differs from the isotropic one. Consequently, the development of optical devices based on color centers requires a sufficient increase of their brightness, which implies the increase of both emission rate and collection efficiency.

Conventionally, the emission rate of color centers can be enhanced by exploiting the Purcell effect, which manifests itself as a modification of emission properties, when an emitter is placed in the vicinity of a cavity with a resonant frequency that coincides with the ZPL of the color center [9]. High emission rate is usually achieved either by using plasmonic cavities that are characterized by ultrasmall mode volume, or dielectric cavities that can be designed to have very large quality factors (Q -factors) [10]. In the plasmonic structures [11–13], the strength of the Purcell effect, however, substantially depends on the position of the emitter, and strong Ohmic losses in metals may result in low radiation efficiency. Therefore, most of the studies are focused on coupling color centers to dielectric cavities, which can be divided into two main groups based on the type of the considered geometry.

The first one relies on color centers embedded in bulk diamond or diamond films. A scenario of their interaction with dielectric cavities is realized by fabrication of the resonant structures from the diamond itself [14–19]. Although such an approach allows for the control over the orientation of the color center symmetry axis, it is not very common, because fabrication of high-quality diamond nanostructures presents major technological difficulties [9,14].

In this study, we focus on the second type of diamond-based sources in the form of small diamond nanoparticles with the size of several tens of nanometers containing single or multiple defects. Such nanoparticles can be experimentally tested after the fabrication, and then the ones with the desired properties (e.g., containing a single defect

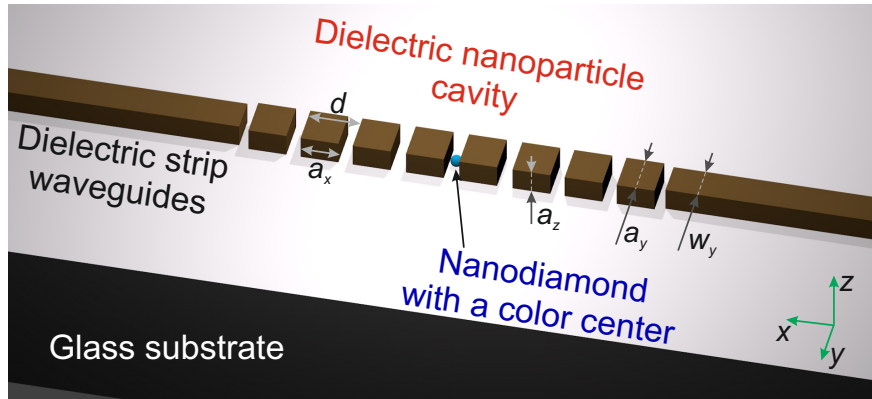


FIG. 1. (a) Scheme of the considered structure: a diamond nanoparticle with an embedded color center is placed in the middle of the cavity formed by dielectric particles with high refractive index. The single-mode homogeneous dielectric waveguides butt-coupled to the cavity serve as channels for efficient photon extraction. Parameters of the system are given in the text

with high quantum efficiency and absence of photo-bleaching) can be placed at the appropriate position using different techniques [11, 13, 20–22], usually by a pick-and-place method with atom-force microscopy tip. Coupling of an emitter in a diamond nanoparticle to a dielectric cavity is usually achieved by placing it on the surface of a dielectric cavity [20, 21, 23–26]. In this case, however, the interaction occurs only via evanescent tails of the cavity field, which is far from ideal, because the electric field in dielectric cavities is typically concentrated inside the dielectric material. Therefore, one of the specific problems is to design a proper cavity that will ensure its efficient interaction with a color center embedded in a nanodiamond located in such structure [27].

Another important problem is the efficient collection of the emission from the color centers. Typically, in experiments the emission is collected by using far-field optical microscopes. While this might be a convenient approach for the experiments in a laboratory, for the practical advancement in the scalable photonic and quantum integrated circuits, the more favorable scheme is the coupling of the emission into a mode of a planar single-mode ridge/strip waveguide or a nanowire [28–30]. However, coupling of a defect in a nanodiamond directly to the homogeneous dielectric waveguide or optical fiber is also a quite inefficient process, because similarly to dielectric cavities, coupling occurs only through the evanescent field of a guided mode [22, 31–34].

The approach, exploited in this study, is based on the use of periodic waveguides with high local density of optical guided modes, which provides a substantial increase in the rate of emission that is directed into the waveguide modes. Namely, we consider a system composed of a waveguide-type cavity made of high-refractive-index nanoparticles butt-coupled to a single mode homogeneous optical waveguide (see Fig. 1), that allows improvement of both the ZPL emission rate and the collection efficiency of the emission from the color center in a nanodiamond at the same time. First, we calculate the properties of the designed cavity, then we analyze its coupling with single-mode homogeneous strip waveguide, and after that we discuss the main issues that deteriorate the performance of considered structure and suggest different modifications that can partially restore it.

The designed cavity operates on the quasi-dark mode of the subwavelength array of mutually coupled magnetic dipole resonances of single dielectric nanoparticles with high refractive index [35, 36]. Interaction of a dipole emitter with such cavity is similar to the interaction with photonic-crystal waveguides and is based on the excitation of the slow light guided modes of a periodic system, i.e. modes which are characterized with a group velocity that tends to zero at the edge of the Brillouin zone and, consequently, a high density of optical states [37]. Photonic crystal waveguides, however, exhibit maximum field distribution of the guided mode inside the dielectric layer [38], which is the reason why such structures work well for emitters embedded inside the waveguide slab [19, 39]. In contrast, the cavity suggested in this work, interacts efficiently with emitters placed in the gap between the dielectric particles. This can be seen from the calculated dispersion of the infinite periodic system along with the field distribution of the corresponding mode, shown in Fig. 2(a-c) for the following parameters of the system: dimensions of the particles $a_x = 160$ nm, $a_y = 180$ nm, $a_z = 100$ nm, material of the particles is lossless dielectric with $\varepsilon = 14$, period of the structure $d = 225$ nm, and the refractive index of the substrate is $n = 1.45$. All numerical simulations were performed in a commercial software Computer Simulation Technology (CST). Fig. 2(a) shows that the dispersion of the fundamental waveguide mode is characterized by zero group velocity and, consequently, with the Purcell factor (PF) that diverges near the frequency ≈ 410 THz. Calculation of the PF, defined as the emission rate of a point-like

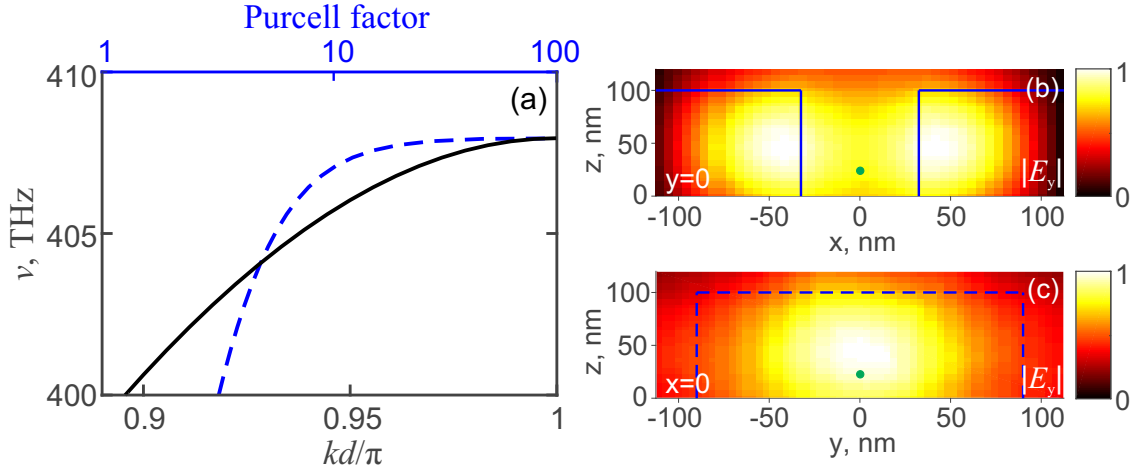


FIG. 2. (a) Dispersion diagram of an infinite periodic (in x direction) chain of cubic nanoparticles (bottom horizontal axis) and Purcell factor (PF) (top horizontal axis in logarithmic scale) calculated for the source placed in the infinite periodic system at the point shown with a green circle in (b,c); k is the Bloch wavenumber, d is the period of the array. (b,c) Distribution of the y -component of electric field in the single unit cell for the eigenmode at the edge of the Brillouin zone in the plane (b) $x = 0$, (c) $z = 0$. Blue lines indicate the position of the dielectric nanoparticles. Geometrical parameters of the system are given in the text

dipole normalized by the emission rate of the same source in vacuum, was performed based on the eigenmode field distribution [37], assuming that a dipole is placed exactly in the middle of the gap between the particles at the distance of 25 nm above the substrate and its orientation coincides with the orientation of the electric field of the excited mode. From Figs. 2(b,c) we can notice that the interaction of the electric dipole source with such waveguide mode is strong when it is placed between the two central particles. Since the gap between the particles in our calculations was equal to 65 nm, the arrangement is particularly suitable for placing a nanodiamond with a size of 30-50 nm in it.

Further, we calculate the properties of the finite-size structure, shown in Fig. 1. In order to extract the radiation from such a cavity it was butt-coupled to homogeneous strip waveguides with the same height $a_z = 100$ nm and different width $w_y = 130$ nm and made from the same material as the nanoparticles. The size of a homogeneous waveguide was chosen so that the propagation constant of its mode coincides with the propagation constant of the periodic waveguide-cavity. In calculations we assume that an electric dipole source is oriented in y direction and located in the center of spherical diamond nanoparticle (refractive index $n = 2.4$) with radius $r_{ND} = 25$ nm, which is, in turn, placed on the substrate between the two middle particles.

The distribution of the power flow in the investigated structure is schematically shown in Fig. 3(a). In the absence of material losses, the main characteristics are determined by the β -factor, defined as the power emitted into the modes of the strip waveguides P_{WG} normalized by the total power emitted by the source $P_{tot} = P_{WG} + P_{fs}$ (where P_{fs} is the power emitted into free space or substrate), and by the PF, defined here as the power emitted by the point dipole in the structure P_{tot} divided by the power emitted by the same source in the nanodiamond in vacuum P_0 . Such characteristics calculated for the system with 24 particles are presented in Fig. 3(b,c) with solid black curves, respectively. The arrangement allows for almost 40-fold enhancement of the power emitted by the source, while at the same time almost 90% of this power is directed into the modes of the strip waveguides. The quality factor of the structure consisting of 24 particles was ≈ 300 , with the linewidth ≈ 2 nm. At low temperature, the ZPL of color centers can be very narrow (close to the transform-limited line), and the interaction strength can be further increased by implementing a composition of larger number of particles and consequently higher Q -factor. The parameters of the considered structure were tuned in such a way that the finite size system exhibits a resonance at the wavelength ≈ 737 nm, which corresponds to the ZPL of the SiV^- color centers in diamond [8]. However, we emphasize that the proposed dielectric structure can be easily tuned to the desired wavelength by adjusting the geometrical parameters. An example of the scheme designed for the NV^- centers is considered further.

In the basic symmetric arrangement in Fig. 1 photons are emitted in both directions. A unidirectional emission can be straightforwardly achieved by placing a Bragg mirror on one of the sides of the structure. The Bragg reflector consisted of 10 particles (in order to ensure the sufficient reflection coefficient) with adjusted width a_y . Since the Bloch wavelength of the periodic waveguide is close to $2d$, the reflected wave should be almost in-phase with the emitted

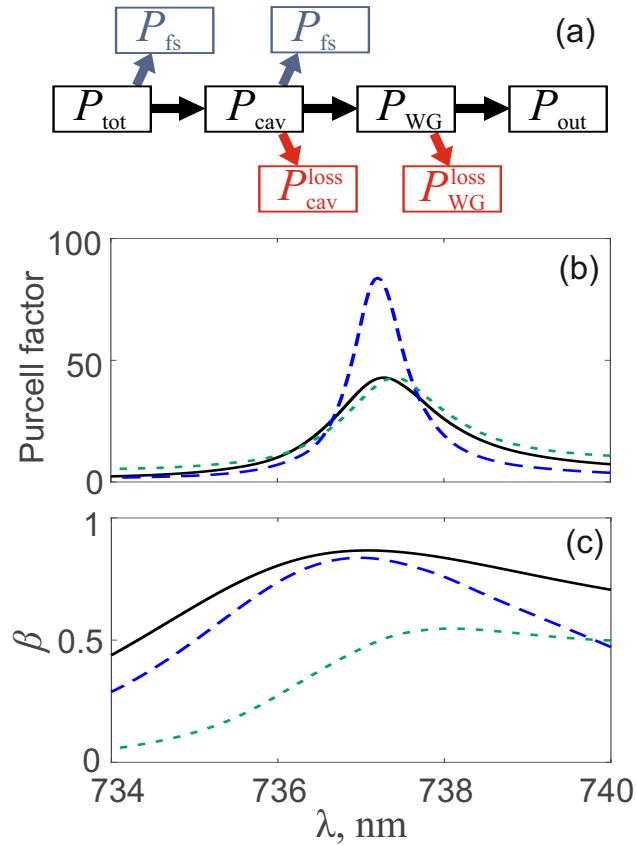


FIG. 3. (a) Power flow distribution in the considered system. (b) Purcell factor and (c) β -factor calculated for the finite structure shown in Fig. 1 made of material with permittivity $\varepsilon = 14$. Solid black curve corresponds to the symmetric arrangement, long-dashed blue curves correspond to the design with Bragg reflector put on one of the sides of the structure, and short-dashed green curves – to the system composed of two structures rotated by $\pi/2$ angle in the plane of substrate with respect to each other. Geometrical parameters of the structure are given in the text

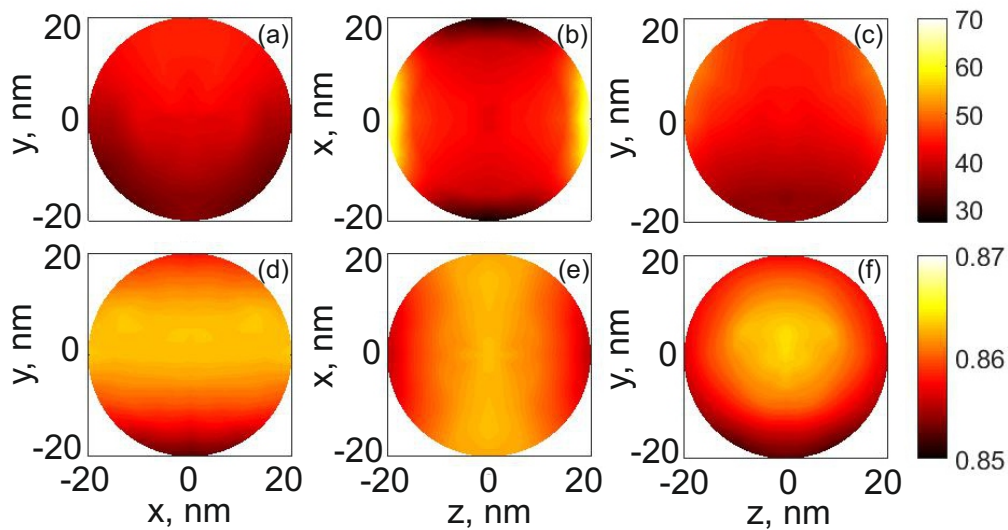


FIG. 4. (a-c) Purcell factor and (d-f) β -factor calculated for different positions of the dipole source within the nanodiamond in (a,d) $x = 0$ plane, (b,e) $y = 0$ plane, (c,f) $z = 0$ plane

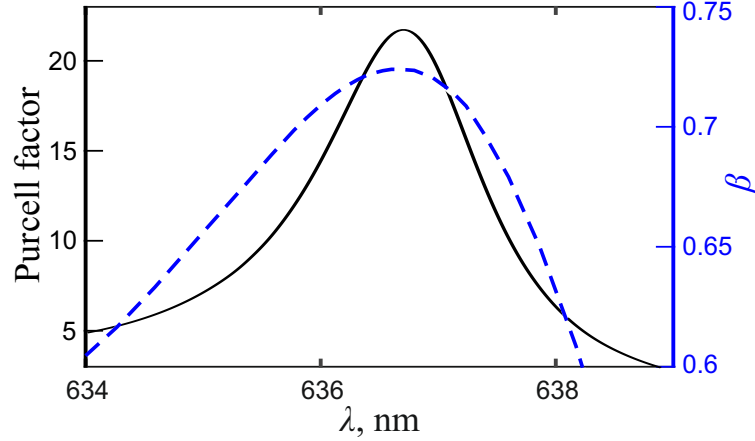


FIG. 5. Purcell factor (left vertical axis) and β -factor (right vertical axis) for the structure shown in Fig. 1 made of gallium phosphide with real part of permittivity $\varepsilon = 10.95$ and zero imaginary part; other parameters are given in the text. The operational wavelength of the structure matches the ZPL transition of NV^- color centers ≈ 637 nm

one, regardless of the number of particles in the cavity. The calculated PF and β factor for the system with reflector, shown in Fig. 3(b,c) with dashed blue curves, confirm this: the power emitted by the source has almost doubled, while approximately the same fraction $\approx 85\%$ is channeled into one remaining strip waveguide. This can be potentially beneficial for the development of scalable quantum optical circuits with different elements connected via single-mode dielectric strip waveguides. The extraction of propagating photons from the nanowaveguide with high efficiency can be achieved by well-established methods of far-field [40] or nanowaveguide/fiber [41] grating out-coupling.

There are several main factors that can substantially affect the performance of considered structure, including position of the source, orientation of its dipole moment, and material losses in dielectric. One of the essential issues is related to the orientation of the dipole source. In fact, the designed system works well only for the y -oriented source. Therefore, if, for example, the symmetry axis of the NV^- center in a nanodiamond placed inside the structure happens to be oriented along the y direction, its dipole moment can be oriented either along x or along z direction. Consequently, the coupling of such source to the cavity mode vanishes. In order to overcome this problem, we consider a “2D” structure, that is composed of two considered “1D” structures shown in Fig. 1, one of which is rotated by 90 degrees in $x - y$ plane, thus achieving identical performance characteristics for arbitrary orientation of a dipole source in the plane of the substrate. Because the gap between the particles is small as compared to their width, four central particles become noticeably overlapped with each other, which leads to overall decreased performance of the structure. In order to restore approximately the same value of Q -factor and PF as for the “1D” structure, we have increased the number of particles in the system to 36 and have slightly adjusted the four central particles by changing a_x from 160 to 150 nm. The results of calculations show that such “2D” structure with 36 particles maintains the same Q -factor and PF as “1D” structure [see black solid and green dashed curves in Fig. 3(b)]. Although the β -factor has dropped down to $\approx 50\%$ [green dashed curves in Fig. 3(c)], in this geometry all characteristics remain the same for any orientation of the dipole source in $x - y$ plane.

Further, we consider the effect of small deviations of the position of the source on the emission and extraction efficiency. The change in the PF is determined mainly by the interaction with the cavity mode, in which strength is proportional to the electric field intensity at the point of the source location. According to eigenmode calculations shown in Fig. 2(b,c), the dependence is quite weak. We have confirmed this by performing the exact numerical calculations for the finite system. Colormaps plotted in Figs. 4(a-c) show the values of PF for different positions of the color center at the distances up to 20 nm from the center of the nanodiamond in $x - y$ and $x - z$ and $y - z$ planes. The variation of PF is observed only in the range from $\approx 30 - 60$, which shows that for almost arbitrary position of a defect in a nanodiamond the emission rate remains as high as in the center.

The similar maps in Figs. 4(d-f) show the dependence of β -factor on the position of the dipole source. Since in the absence of losses in the system β -factor is determined as $\beta = P_{WG}/(P_{fs} + P_{WG})$ (see Fig. 3(a)), it can be modified in two ways. First, the decrease (increase) of PF reduces (enhances) the β -factor directly. And, second, the increase of P_{FS} , which occurs when the dipole source gets closer to the substrate [42], also reduces β -factor. The combination of these two factors gives the result shown in Figs. 4(d-f). Overall, we can expect approximately the same characteristics of the system (PF and β -factor) for almost arbitrary position of the color center in the small nanodiamond (40–50 nm).

We stress here that because the optical size of a nanodiamond is much smaller than the wavelength, its form and size also do not noticeably affect emission properties [27, 43]. We also note, that further tolerance to the position of the emitter can be achieved by designing a similar structure with smaller height a_z . Our calculations show (not presented here) that e.g. for $a_z = 50$ nm field distribution in the gap between the particles becomes even more homogeneous, and, consequently, dependence of emission properties on the position becomes even more negligible.

Finally, we consider the effect of material losses in the system. For instance, crystalline silicon, the most exploited material with high refractive index at visible frequency range, has an imaginary part of permittivity of about 0.065 at the wavelength $\lambda \approx 737$ nm [44]. Our calculations revealed that taking into account the material losses in silicon results in following changes. The Q -factor of the resonance and, consequently, the PF and P_{tot} are reduced by ≈ 3 times and the fraction of power lost in the cavity $P_{\text{cav}}^{\text{loss}}/P_{\text{cav}}$ [see Fig. 3(a)] reaches almost 60%. Moreover, the total radiation efficiency also depends on the losses in the strip waveguides $P_{\text{WG}}^{\text{loss}}$, which grow with the increase of the length of the waveguide. E.g. for the $4\mu\text{m}$ -size waveguides we have estimated the radiative PF (P_{out}/P_0) to be only ≈ 10 , while the β -factor (which is defined as $P_{\text{out}}/P_{\text{tot}}$ for the system with losses) dropped down to 10%. For color centers with ZPL at lower wavelengths radiation efficiency is expected to be even lower due to higher losses in silicon.

This problem can be overcome by using different materials with lower losses. E.g. gallium phosphide with refractive index $n \approx 3.5$ or materials with lower refractive index, such as TiO_2 or SiN [45]. To illustrate the possibility of engineering structures tuned at different operational frequencies and fabricated from different materials, we have developed a similar system made from GaP, that is suitable for operation with NV color centers with ZPL at ≈ 637 nm. The numerical simulation results, shown in Fig. 5 demonstrate, that it is indeed possible to have similar values of PF and β for considered structure. In this case the radiation efficiency of this composition is limited only by the internal quantum efficiency of the color center, which in the case of the nanodiamond, can be estimated before the placement in the nanostructure.

In summary, we have proposed a design of a dielectric structure composed of a nanoparticle waveguide-cavity butt-coupled to dielectric strip waveguide for efficient interaction with the color centers embedded in small nanodiamonds with linear size up to ≈ 50 nm. We have studied numerically optical properties of considered arrangement and have shown that it allows one to increase the emission rate of color centers by several orders of magnitude in ≈ 2 nm spectral range and at the same time to provide out-coupling of emission to planar strip waveguide with up to 85% efficiency. We have shown that tuning of the system can be realized in a straight-forward way by adjusting the geometrical parameters of nanostructures, which makes them a promising platform for creating bright single photon sources based on nanodiamonds containing color centers for quantum optical integrated circuits.

Acknowledgements

This work was supported by the Russian Science Foundation Grant No. 17-72-10280. Authors would like to acknowledge D. Zuev and I. Shadrivov for fruitful discussions.

References

- [1] Aharonovich I., Castelletto S., Simpson D.A., Su C.-H., Greentree A.D., Prawer S. Diamond-based single-photon emitters. *Reports on Progress in Physics*, 2011, **74**, P. 076501.
- [2] Aharonovich I., Englund D., Toth M. Solid-state single-photon emitters. *Nature Photonics*, 2016, **10**, P. 631–641.
- [3] Schirhagl R., Chang K., Loretz M., Degen C.L. Nitrogen-Vacancy Centers in Diamond: Nanoscale Sensors for Physics and Biology. *Annual Review of Physical Chemistry*, 2014, **65**, P. 83–105.
- [4] Maze J.R., Stanwix P.L., Hodges J.S., Hong S., Taylor J.M., Cappellaro P., Jiang L., Gurudev Dutt M.V., Togan E., Zibrov A.S., et al. Nanoscale magnetic sensing with an individual electronic spin in diamond. *Nature*, 2008, **455**, P. 644–647.
- [5] Hong S., Grinolds M.S., Pham L.M., Le Sage D., Luan L., Walsworth R.L., Yacoby A. Nanoscale magnetometry with NV centers in diamond. *MRS Bulletin*, 2013, **38**, P. 155–161.
- [6] Kucsko G., Maurer P., Yao N.Y., Kubo M., Noh H., Lo P., Park H., Lukin M.D. Nanometre-scale thermometry in a living cell. *Nature* 2013, **500**, P. 54–58.
- [7] Toyli D.M., de las Casas C.F., Christle D.J., Dobrovitski V.V., Awschalom D.D. Fluorescence thermometry enhanced by the quantum coherence of single spins in diamond. *Proceedings of the National Academy of Sciences*, 2013, **110**, P. 8417–8421.
- [8] Neu E., Hepp C., Hauschild M., Gsell S., Fischer M., Sternschulte H., Steinmüller-Nethl D., Schreck M., Becher C. Low-temperature investigations of single silicon vacancy colour centres in diamond. *New Journal of Physics*, 2013, **5**, P. 043005.
- [9] Aharonovich I., Greentree A.D., Prawer S. Diamond photonics. *Nature Photonics*, 2011, **5**, P. 397–405.
- [10] Pelton M. Modified spontaneous emission in nanophotonic structures. *Nature Photonics*, 2015, **9**, P. 427.
- [11] Schietinger S., Barth M., Aichele T., Benson O. Plasmon-Enhanced Single Photon Emission from a Nanoassembled Metal-Diamond Hybrid Structure at Room Temperature. *Nano Letters*, 2009, **9**, P. 1694–1698.
- [12] Andersen S.K., Kumar S., Bozhevolnyi S.I. Ultrabright Linearly Polarized Photon Generation from a Nitrogen Vacancy Center in a Nanocube Dimer Antenna. *Nano Letters*, 2017, **17**, P. 3889–3895.
- [13] Siampour H., Kumar S., Davydov V.A., Kulikova L.F., Agafonov V.N., Bozhevolnyi S.I. On-chip excitation of single germanium vacancies in nanodiamonds embedded in plasmonic waveguides. *Light: Science & Applications*, 2018, **7**, P. 397–405.

- [14] Bayn I., Meyler B., Lahav A., Salzman J., Kalish R., Fairchild B.A., Praver S., Barth M., Benson O., Wolf T., et al. Processing of photonic crystal nanocavity for quantum information in diamond. *Diamond and Related Materials*, 2011, **20**, P. 937–943.
- [15] Faraon A., Barclay P.E., Santori C., Fu K.-M.C., Beausoleil R.G. Resonant enhancement of the zero-phonon emission from a colour centre in a diamond cavity. *Nature Photonics*, 2011, **5**, P. 301–305.
- [16] Riedrich-Möller J., Kipfstuhl L., Hepp C., Neu E., Pauly C., Mücklich F., Baur A., Wandt M., Wolff S., Fischer M., et al. One- and two-dimensional photonic crystal microcavities in single crystal diamond. *Nature Nanotechnology*, 2012, **7**, P. 69–74.
- [17] Faraon A., Santori C., Huang Z., Acosta V.M., Beausoleil R.G. Coupling of Nitrogen-Vacancy Centers to Photonic Crystal Cavities in Monocrystalline Diamond. *Phys. Rev. Lett.*, 2012, **109**, P. 033604.
- [18] Evans R.E., Sipahigil A., Sukachev D.D., Zibrov A.S., Lukin M.D. Narrow-Linewidth Homogeneous Optical Emitters in Diamond Nanostructures via Silicon Ion Implantation. *Phys. Rev. Applied*, 2016, **5**, P. 044010.
- [19] Sipahigil A., Evans R.E., Sukachev D.D., Burek M.J., Borregaard J., Bhaskar M.K., Nguyen C.T., Pacheco J.L., Atikian H.A., Meuwly C., et al. An integrated diamond nanophotonics platform for quantum-optical networks. *Science*, 2016, **354**, P. 847–850.
- [20] Gregor M., Henze R., Schröder T., Benson O. On-demand positioning of a preselected quantum emitter on a fiber-coupled toroidal microresonator. *Applied Physics Letters*, 2009, **95**, P. 153110.
- [21] Wolters J., Schell A.W., Kewes G., Nüsse N., Schoengen M., Döschner H., Hannappel T., Löchel B., Barth M., Benson O. Enhancement of the zero phonon line emission from a single nitrogen vacancy center in a nanodiamond via coupling to a photonic crystal cavity. *Applied Physics Letters*, 2010, **97**, P. 141108.
- [22] Liebermeister L., Petersen F., Münchow A.V., Burchardt D., Hermelbracht J., Tashima T., Schell A.W., Benson O., Meinhardt T., Krueger A., et al. Tapered fiber coupling of single photons emitted by a deterministically positioned single nitrogen vacancy center. *Applied Physics Letters*, 2014, **104**, P. 031101.
- [23] van der Sar T., Heeres E.C., Dmochowski G.M., de Lange G., Robledo L., Oosterkamp T.H., Hanson R. Nanopositioning of a diamond nanocrystal containing a single nitrogen-vacancy defect center. *Applied Physics Letters*, 2009, **94**, P. 173104.
- [24] Barclay P.E., Santori C., Fu K.-M., Beausoleil R.G., Painter O. Coherent interference effects in a nano-assembled diamond NV center cavity-QED system. *Opt. Express*, 2009, **17**, P. 8081–8197.
- [25] Englund D., Shields B., Rivoire K., Hatami F., Vučković J., Park H., Lukin M.D. Deterministic Coupling of a Single Nitrogen Vacancy Center to a Photonic Crystal Cavity. *Nano Letters*, 2010, **10**, P. 3922–3926.
- [26] Gould M., Schmidgall E.R., Dadgostar S., Hatami F., Fu K.-M.C. Efficient Extraction of Zero-Phonon-Line Photons from Single Nitrogen-Vacancy Centers in an Integrated GaP-on-Diamond Platform. *Phys. Rev. Applied*, 2016, **6**, P. 011001.
- [27] Alagappan G., Krivitsky L.A., Png C.E. Diamond in a Nanopocket: A New Route to a Strong Purcell Effect. *ACS Omega*, 2018, **3**, P. 4733–4742.
- [28] Silverstone J.W., Bonneau D., Ohira K., Suzuki N., Yoshida H., Iizuka N., Ezaki M., Natarajan C.M., Tanner M.G., Hadfield R.H., et al. On-chip quantum interference between silicon photon-pair sources. *Nature Photonics*, 2014, **8**, P. 104–108.
- [29] Lodahl P., Mahmoodian S., Stobbe S. Interfacing single photons and single quantum dots with photonic nanostructures. *Reviews of Modern Physics*, 2015, **87**, P. 347–400.
- [30] Johnson S., Dolan P.R., Smith J.M. Diamond photonics for distributed quantum networks. *Progress in Quantum Electronics*, 2017, **55**, P. 129–165.
- [31] Fu K.-M.C., Santori C., Barclay P.E., Aharonovich I., Praver S., Meyer N., Holm A.M., Beausoleil R.G. Coupling of nitrogen-vacancy centers in diamond to a GaP waveguide. *Applied Physics Letters*, 2008, **93**, P. 234107.
- [32] Schröder T., Fujiwara M., Noda T., Zhao H.-Q., Benson O., Takeuchi S. A nanodiamond-tapered fiber system with high single-mode coupling efficiency. *Opt. Express*, 2012, **20**, P. 10490–10497.
- [33] Liebermeister L. *Photonic Waveguides Evanescently Coupled with Single NV-centers*. Fakultät für Physik der Ludwig-Maximilians-Universität München, 2015.
- [34] Fujiwara M., Neitzke O., Schröder T., Schell A.W., Wolters J., Zheng J., Mouradian S., Almqvist M., Takeuchi S., Englund D., et al. Fiber-Coupled Diamond Micro-Waveguides toward an Efficient Quantum Interface for Spin Defect Centers. *ACS Omega*, 2017, **2**, P. 7194–7202.
- [35] Krasnok A., Glybovski S., Petrov M., Makarov S., Savelev R., Belov P., Simovski C., Kivshar Y. Demonstration of the enhanced Purcell factor in all-dielectric structures. *Applied Physics Letters*, 2016, **108**, P. 211105.
- [36] Savelev R.S., Sergaeva O.N., Baranov D.G., Krasnok A.E., Alù A. Dynamically reconfigurable metal-semiconductor Yagi-Uda nanoantenna. *Phys. Rev. B*, 2017, **95**, P. 235409.
- [37] Yao P., Manga Rao V., Hughes S. On-chip single photon sources using planar photonic crystals and single quantum dots. *Laser & Photonics Reviews*, 2010, **4**, P. 499–516.
- [38] Javadi A., Mahmoodian S., Söllner I., Lodahl P. Numerical modeling of the coupling efficiency of single quantum emitters in photonic-crystal waveguides. *J. Opt. Soc. Am. B*, 2018, **35**, P. 514–522.
- [39] Arcari M., Söllner I., Javadi A., Lindskov Hansen S., Mahmoodian S., Liu J., Thyrrerstrup H., Lee E.H., Song J.D., Stobbe S., et al. Near-Unity Coupling Efficiency of a Quantum Emitter to a Photonic Crystal Waveguide. *Phys. Rev. Lett.*, 2014, **113**, P. 093603.
- [40] Wang Y., Wang X., Flueckiger J., Yun H., Shi W., Bojko R., Jaeger N.A.F., Chrostowski L. Focusing sub-wavelength grating couplers with low back reflections for rapid prototyping of silicon photonic circuits. *Opt. Express*, 2014, **22**, P. 20652–20662.
- [41] Zhu L., Yang W., Chang-Hasnain C. Very high efficiency optical coupler for silicon nanophotonic waveguide and single mode optical fiber. *Opt. Express*, 2017, **25**, P. 18462–18473.
- [42] Novotny L., Hecht B. *Principles of Nano-optics*. Cambridge University Press, New York, 2006.
- [43] Rogobete L., Schniepp H., Sandoghdar V., Henkel C. Spontaneous emission in nanoscopic dielectric particles. *Opt. Lett.*, **2003**, **28**, P. 1736–1738.
- [44] Green M.A. Self-consistent optical parameters of intrinsic silicon at 300K including temperature coefficients. *Solar Energy Materials and Solar Cells*, 2008, **92**, P. 1305–1310.
- [45] Baranov D.G., Zuev D.A., Lepeshov S.I., Kotov O.V., Krasnok A.E., Evlyukhin A.B., Chichkov B.N. All-dielectric nanophotonics: the quest for better materials and fabrication techniques. *Optica*, 2017, **4**, P. 814–825.